

# Kirkwood-Dirac Nonpositivity is a Necessary Resource for Quantum Computing

Jonathan J. Thio,<sup>1</sup> Songqinghao Yang,<sup>1,2</sup> Stephan De Bièvre,<sup>3</sup>  
Crispin H. W. Barnes,<sup>1</sup> and David R. M. Arvidsson-Shukur<sup>2</sup>

<sup>1</sup>*Cavendish Lab., Department of Physics, Univ. of Cambridge, Cambridge CB3 0HE, UK*

<sup>2</sup>*Hitachi Cambridge Lab., J.J. Thomson Avenue, Cambridge CB3 0HE, UK*

<sup>3</sup>*Univ. Lille, CNRS, Inria, UMR 8524, Laboratoire Paul Painlevé, F-59000 Lille, France*

(Dated: September 18, 2025)

Classical computers can simulate models of quantum computation with restricted input states. The identification of such states can sharpen the boundary between quantum and classical computations. Previous works describe simulable states of odd-dimensional systems. Here, we further our understanding of systems of qubits. We do so by casting a real-quantum-bit model of computation in terms of a Kirkwood-Dirac (KD) quasiprobability distribution. Algorithms, throughout which this distribution is a proper (positive) probability distribution can be simulated efficiently on a classical computer. We leverage recent results on the geometry of the set of KD-positive states to construct previously unknown classically-simulable (bound) states. Finally, we show that KD nonpositivity is a resource monotone for quantum computation, establishing KD nonpositivity as a necessary resource for computational quantum advantage.

*Introduction:*—Current efforts in quantum-computing research are motivated by the expectation that quantum computers’ power will exceed that of their classical counterparts. However, identifying exactly the source of quantum advantage is notoriously difficult. A deepened knowledge on this topic is crucial to enable the full power of quantum computing.

One may investigate the source of quantum advantage by comparing a universal model of quantum computation with a suitably restricted model. A widely used universal model of quantum computation is the quantum-computation-by-state-injection model [1], consisting of arbitrary single-qubit state preparations, application of Clifford gates, and computational-basis measurements. One can restrict this model by reducing its set of input states. If the restricted model admits efficient classical simulation, then (if quantum advantages do indeed exist), the excluded states are necessary for quantum speedup.

This approach is exemplified by the Gottesman-Knill (GK) theorem [2], which shows that the GK model of computation—a model restricted to stabilizer-state preparations (defined below), Clifford gates, and computational-basis measurements—can be simulated efficiently on classical hardware. Consequently, access to *magic* states—states that cannot be written as mixtures of stabilizer states—is necessary for quantum advantage. This suggests that magic states are the key resource that enables quantum advantage in the quantum-computation-by-state-injection model. In support of this conclusion, it has been proven that there exist *distillable* [1, 3] magic states that, when appended to the GK model, allow for efficient reproduction of any quantum computation by state injection. However, not all magic states are distillable. Within the GK model, there exist *bound* magic states—magic states that still yield a classically simulable model when combined with the GK model [4, 5]. Characterizing the geometry of bound magic states

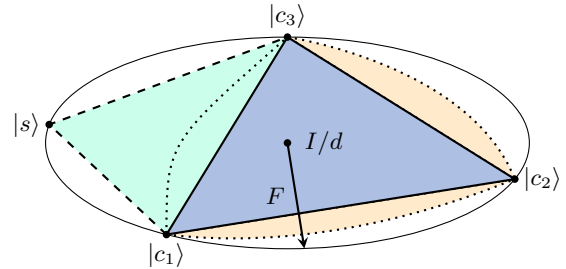


FIG. 1. **Schematic Overview of the Geometry of Simulable States.** The disc represents the set of all 2-qubit states, with pure states on the boundary. The states  $|c_j\rangle$  and  $|s\rangle$  are CSS and non-CSS stabilizer states, respectively. The area bounded by the solid triangle defines the CSS polytope. Further stabilizer mixtures are found in the area bounded by the dashed lines. The shape enclosed by the dotted line is the set of  $\mathbb{Z}_2^n$ -KD-positive states. The states highlighted in yellow are  $\mathbb{Z}_2^n$ -KD positive but lie outside the stabilizer polytope: they are bound magic states for the DGBR model.

pushes the reach of classical simulation algorithms, allowing us to sharpen the boundary between classical and quantum computation.

The main tools for identifying bound magic states are quasiprobability distributions—mathematical objects resembling probability distributions, but which may assume values outside the interval  $[0, 1]$ . For certain *positive* states, however, the quasiprobability distribution lies entirely within  $[0, 1]$  and thus is a proper probability distribution. Many algorithms enable efficient classical simulations of different models of quantum computation if the input state is positive with respect to some specific quasiprobability distributions [5–16]. Consequently, positive states can be identified as simulable states. A positive state that is not a stabilizer mixture must be a bound magic state.

The most prominent example of a quasiprobability-

based simulation algorithm uses Gross’ Wigner function [5, 17]. This quasiprobability distribution has a rich structure, leading to a broadly applicable simulation algorithm. Unfortunately, Gross’ Wigner function is only defined for systems of odd Hilbert-space dimensionality: the construction does not apply to qubits—the most widely used components in modern quantum-information processing. This limitation was subsequently addressed in Refs. [11–15, 18]. In particular, Ref. [18] introduced a quasiprobability distribution tailored to a computational model defined on *rebits* (qubits represented by real density matrices) [19]. We refer to this model as the Delfosse–Guerin–Bian–Raussendorf (DGBR) model; we refer to the associated quasiprobability representation as the DGBR distribution. The DGBR distribution leads to an efficient classical simulation algorithm for circuits with input states with positive DGBR distributions [18].

In this Article, we further our knowledge of classical simulability of quantum computers through the lens of Kirkwood-Dirac (KD) distributions—a trending family of quasiprobability distributions [20–22]. We begin by generalizing the DGBR distribution to a complex-valued distribution, which we identify as a KD distribution. We show that this generalization preserves all of the properties relevant to simulation, implying that our KD distribution’s positive input states are efficiently classically simulable in the DGBR model. This allows us to use the powerful toolkit developed for the characterization of the set of KD-positive states to study classical simulability [23–25]. In doing so, we characterize the geometry of the KD-positive states (see Fig. 1) and discover a substantial volume of previously unknown bound magic states for the DGBR model. Compared to the GK theorem, we extend the volume of simulable 2-qubit states by 15%. Finally, we define the KD mana, a measure of the total nonpositivity of our KD distribution. The KD mana, we show, is an additive monotone for the resource theory of rebit quantum computation. Thus, we establish KD nonpositivity as a necessary resource for quantum-computational advantage. We use this result to lower bound the efficiency of any (including magic) distillation protocol on rebits.

*Preliminaries:*—Throughout this paper, we consider a system of  $n$  qubits with states in the Hilbert space  $\mathcal{H} = (\mathbb{C}^2)^{\otimes n}$  of dimensionality  $d = 2^n$ , and denote the set of density matrices on  $\mathcal{H}$  by  $\mathcal{D}(\mathcal{H})$ . We say that a density matrix  $\rho \in \mathcal{D}(\mathcal{H})$  is real, and thus a rebit state, if and only if its elements are real in the computational basis. We will index elements of  $d \times d$  matrices by binary vectors  $\mathbf{u}, \mathbf{v} \in \mathbb{Z}_2^n$ . Furthermore, we let  $Z_j$  denote Pauli- $Z$  on the  $j$ th qubit and identity everywhere else. We define  $X_k$  similarly. We denote the real Pauli string associated with  $\mathbf{u}, \mathbf{v}$  by

$$P_{\mathbf{u}, \mathbf{v}} = \prod_{j=1}^n Z_j^{v_j} X_j^{u_j}. \quad (1)$$

In this work, stabilizer states, and in particular the Calderbank-Shor-Steane (CSS) stabilizer states [26–28] will play a central role. Stabilizer states are unique  $+1$  eigenstates of a maximal commuting subgroup of the Pauli group [29]. The CSS stabilizer states are the stabilizer states that have a maximal stabilizing subgroup of the form  $\langle S_Z \cup S_X \rangle$ , where  $S_Z$  and  $S_X$  are stabilizing subgroups consisting only of elements of the form  $P_{\mathbf{0}, \mathbf{v}}$  and  $P_{\mathbf{u}, \mathbf{0}}$ , respectively. Here,  $\langle \dots \rangle$  denotes the group generated by the bracketed elements. The CSS states form the logical basis of the popular CSS error-correction codes [26–28].

The convex mixtures of the stabilizer, rebit-stabilizer, and CSS states form polytopes in  $\mathcal{D}(\mathcal{H})$ . (See Fig. 1.) We refer to these polytopes as the stabilizer, rebit-stabilizer, and CSS polytopes, and we refer to states inside these polytopes as stabilizer, rebit-stabilizer, and CSS mixtures, respectively. The stabilizer polytope contains the rebit-stabilizer polytope, and the rebit stabilizer polytope contains the CSS polytope.

*The DGBR Model and Distribution:*—We now consider an  $n$ -rebit model of computation of particular relevance to the implementation of error-corrected surface codes [30]. Let  $H$  denote the Hadamard gate and let  $\text{CNOT}_{ct}$  denote a CNOT gate with qubit  $c$  as control and qubit  $t$  as target.

**Definition 1 (DGBR Model).** *The DGBR model allows for the following operations:*

- Initialization of qubits in CSS states.
- Application of  $H^{\otimes n}$ ,  $\text{CNOT}_{ct}$  or  $P_{\mathbf{u}, \mathbf{v}}$  to the qubits.
- Measurement of any qubit in the computational basis.

*Previous measurement outcomes may determine future operations adaptively.*

Via the GK theorem, the DGBR model is efficiently simulable on a classical computer. Like the quantum-computation-by-state-injection model, the DGBR model can efficiently reproduce any other gate-based quantum computation if also given access to arbitrary real input states  $\rho_{\text{input}}$ . However, there exists a broad class of input states which still permit classical simulability. What states are efficiently simulable is studied through the DGBR distribution  $W : \mathcal{D}(\mathcal{H}) \rightarrow \mathbb{R}^{d \times d}$  [18]. The DGBR distribution is defined as

$$W_{\mathbf{u}, \mathbf{v}}(\rho) = \text{Tr}(A_{\mathbf{u}, \mathbf{v}} \rho), \quad (2)$$

where the phase-space point operators of the DGBR distribution are

$$A_{\mathbf{u}, \mathbf{v}} = P_{\mathbf{u}, \mathbf{v}} A_{\mathbf{0}, \mathbf{0}} P_{\mathbf{u}, \mathbf{v}}^\dagger \quad \text{and} \quad A_{\mathbf{0}, \mathbf{0}} = \sum_{\mathbf{u}, \mathbf{v} = \mathbf{0} \pmod{2}} \frac{P_{\mathbf{u}, \mathbf{v}}}{2^{2n}}. \quad (3)$$

The DGBR distribution possesses several properties important to simulation. Specifically, its positive real pure states coincide with the CSS states; it transforms covariantly under the unitary operations in the DGBR model; and it satisfies a natural product rule with respect to tensor products. Using these properties, Ref. [18] showed that as long as  $\rho_{\text{input}}$  is DGBR positive, then an efficient classical algorithm simulates the DGBR model even when given access to  $\rho_{\text{input}}$  [18].

*The  $\mathbb{Z}_2^n$ -Kirkwood-Dirac Distribution:*—We now generalize the DGBR distribution to a KD distribution. The KD distributions [20–22, 31] are a family of quasiprobability distributions that have recently been shown to have many applications in various fields including quantum metrology [32–34], quantum foundations [24, 35–41], quantum thermodynamics [42–47], and information scrambling [42, 48–50]. The KD distribution  $Q : \mathcal{D}(\mathcal{H}) \rightarrow \mathbb{C}^{d \times d}$  is defined with respect to two orthonormal bases  $\mathcal{A}$  and  $\mathcal{B}$  for  $\mathcal{H}$ .

We choose  $\mathcal{A}$  and  $\mathcal{B}$  to be tensor products of the eigenstates of the Pauli- $Z$  and  $-X$  operators, respectively. We describe the resulting KD distribution as a special case of the general KD distribution for a finite Abelian group  $G$ , constructed in Ref. [25]. This group structure is crucial for our results. Since we consider  $n$  qubits, a natural choice of  $G$  is  $\mathbb{Z}_2^n$ . We denote the group's elements by  $\mathbf{g} = (g_1, g_2, \dots, g_n)$ , where  $g_j \in \{0, 1\}$ , and the group operation by  $+$ . We fix  $\mathcal{A}$  to be the computational basis  $\{|\mathbf{g}^{(z)}\rangle\}_{\mathbf{g} \in G}$ . Further, we consider the character group of  $G$  denoted by  $\hat{G}$ , for which we also denote the group operation by  $+$ .  $G$  and  $\hat{G}$  play roles similar to position and momentum spaces of continuous-variable systems. As momentum is both a vector and a translation operator, a character  $\chi \in \hat{G}$  is both a vector  $\chi = (\chi_1, \chi_2, \dots, \chi_n)$ , where  $\chi_k \in \{0, 1\}$ , and a function on  $G$ :  $\chi(\mathbf{g}) = \prod_{j=1}^n (-1)^{\chi_j g_j}$ . Using the characters, we define the states

$$|\chi^{(x)}\rangle := \frac{1}{|G|^{1/2}} \sum_{\mathbf{g} \in G} \chi(\mathbf{g}) |\mathbf{g}^{(z)}\rangle, \quad (4)$$

where  $|G|$  denotes the number of elements in the group. Further, we set our second orthonormal basis to be  $\mathcal{B} = \{|\chi^{(x)}\rangle\}_{\chi \in \hat{G}}$ .

The KD distribution of a state  $\rho$  with respect to these choices for  $\mathcal{A}$  and  $\mathcal{B}$  is

$$Q_{\mathbf{g}, \chi}(\rho) = \text{Tr}(B_{\mathbf{g}, \chi} \rho), \quad (5)$$

where

$$B_{\mathbf{g}, \chi} = |\chi^{(x)}\rangle \langle \chi^{(x)} | \mathbf{g}^{(z)} \rangle \langle \mathbf{g}^{(z)} | \quad (6)$$

are the phase-space point operators of the  $\mathbb{Z}_2^n$ -KD distribution. Since  $\langle \mathbf{g}^{(z)} | \chi^{(x)} \rangle \neq 0$ , this KD distribution is informationally complete:  $Q_{\mathbf{g}, \chi}(\rho)$  uniquely defines  $\rho$

[22]. We also consider the KD symbol [22] of an arbitrary generalized measurement

$$\tilde{Q}_{\mathbf{g}, \chi}(E_l) = \frac{\text{Tr}(B_{\mathbf{g}, \chi} E_l)}{|\langle \mathbf{g}^{(z)} | \chi^{(x)} \rangle|^2}. \quad (7)$$

Here,  $\{E_l\}_l$  is the set of positive semidefinite matrices representing a generalized measurement [29]. The KD distribution of a time-evolving state, together with the KD symbol of a generalized measurement, give a complete description of an experiment. The outcome probabilities are calculated using the overlap formula [22, 25]:

$$\text{Tr}(E_l \rho) = \sum_{\mathbf{g}, \chi} \tilde{Q}_{\mathbf{g}, \chi}(E_l) Q_{\mathbf{g}, \chi}(\rho). \quad (8)$$

We now show that the  $\mathbb{Z}_2^n$ -KD distribution is indeed a generalization of the DGBR distribution and enjoys similar simulation properties.

**Theorem 1.** *The  $\mathbb{Z}_2^n$ -KD distribution has the following properties:*

1. (*DGBR Connection*) *The real part of the  $\mathbb{Z}_2^n$ -KD distribution [51] coincides with the DGBR distribution:*

$$\text{Re}[Q_{\mathbf{g}, \chi}(\rho)] = W_{\mathbf{g}, \chi}(\rho). \quad (9)$$

2. (*Hudson's Theorem*) *A pure state is KD positive if and only if it is a CSS state.*
3. (*Covariance*) *The following covariance relationships hold:*

$$Q_{\mathbf{g}_0, \chi_0}(P_{\mathbf{g}, \chi} \rho P_{\mathbf{g}, \chi}^\dagger) = Q_{\mathbf{g}_0 + \mathbf{g}, \chi_0 + \chi}(\rho), \quad (10)$$

$$Q_{\mathbf{g}, \chi}(\mathbb{H}^{\otimes n} \rho \mathbb{H}^{\otimes n \dagger}) = \overline{Q_{\chi, \mathbf{g}}(\rho)}, \quad (11)$$

$$Q_{\mathbf{g}, \chi}(\text{CNOT}_{ct} \rho \text{CNOT}_{ct}^\dagger) = Q_{A_{ct} \mathbf{g}, B_{ct} \chi}(\rho), \quad (12)$$

where  $(A_{ct})_{jk} := \delta_{jk} + \delta_{tj} \delta_{ck}$ ,  $(B_{ct})_{jk} := \delta_{jk} + \delta_{cj} \delta_{tk}$  and the overbar denotes complex conjugation.

4. (*Products*) *Consider a tensor product factorization of  $\mathcal{H} = \mathcal{H}_1 \otimes \mathcal{H}_2$ , and let  $\rho_1 \in \mathcal{D}(\mathcal{H}_1)$  and  $\rho_2 \in \mathcal{D}(\mathcal{H}_2)$ . Then,*

$$Q_{(\mathbf{g}, \mathbf{g}'), (\chi, \chi')}(\rho_1 \otimes \rho_2) = Q_{\mathbf{g}, \chi}(\rho_1) Q_{\mathbf{g}', \chi'}(\rho_2). \quad (13)$$

To prove Theorem 1.1, we first show that the phase-space point operators of the DGBR and  $\mathbb{Z}_2^n$ -KD distributions are connected through

$$A_{\mathbf{g}, \chi} = \frac{1}{2}(B_{\mathbf{g}, \chi} + B_{\mathbf{g}, \chi}^\dagger). \quad (14)$$

Substituting Eq. (14) into Eq. (2) then yields the desired result. We give the details of this proof in Supplemental Note I.

The original Hudson’s theorem [52] determines all pure positive states of the continuous-variable Wigner function [53]. The proof of our version of Hudson’s Theorem for the  $\mathbb{Z}_2^n$ -KD distribution builds on a recent result [25]: all pure KD-positive states of KD distributions based on a finite Abelian group  $G$  are of the form

$$|H; \mathbf{g}, \boldsymbol{\chi}\rangle := \frac{1}{|H|^{1/2}} P_{\mathbf{g}, \boldsymbol{\chi}} \sum_{\mathbf{h} \in H} |\mathbf{h}^{(z)}\rangle. \quad (15)$$

Here,  $H$  is any subgroup of  $G$ . Proving Theorem 1.2 reduces to showing that states of the form in Eq. (15) are CSS states and that all CSS states are of this form. In Supplemental Note II, we confirm these two statements by computing the maximal stabilizing subgroup of the state in Eq. (15).

Covariance Relationship (10) follows directly from Eq. (29) in Ref. [25]. One proves Covariance Relationships (11) and (12) by evaluating the left-hand sides and using the fact that  $H$  and CNOT map eigenstates of real Pauli operators to eigenstates of real Pauli operators. For completeness, we give the details of this calculation in Supplemental Note III.

Last, Theorem 1.4 is immediate.

*Efficient Classical Simulation and Bound Magic States:*—We now identify KD-positive states that are not in the stabilizer polytope, and therefore bound magic states for the DGBR model (Fig. 1). A trivial yet important corollary of Theorem 1.1 is that any KD-positive state must also be DGBR-positive. Since DGBR-positive input states are efficiently classically simulable, a DGBR model is efficiently simulable even if given access to an arbitrary KD-positive input state  $\rho_{\text{input}}$ . For completeness, we provide a KD rephrasing of the DGBR simulation algorithm in Supplemental Note IV.

We now turn to the identification of bound magic states for the DGBR model. We do so using the extensive tools developed to characterize sets of KD-positive states [23, 25, 54]. Theorem 1.1.i of Ref. [23] shows that the only single-qubit KD-positive states are the mixtures of  $|g^{(z)}\rangle \langle g^{(z)}|$  and  $|\chi^{(x)}\rangle \langle \chi^{(x)}|$ . Since these states are all the single-qubit rebit-stabilizer states, the DGBR simulation algorithm can simulate the same set of DGBR circuits with real single-qubit input states as the GK algorithm. Thus, one cannot use our KD distribution to identify potential single-qubit bound states within the DGBR model.

Nevertheless, recent work shows that the set of KD-positive states has a richer structure in higher dimensions: there exist *exotic* KD-positive mixed states that are not mixtures of KD-positive pure states [23]. This applies to the  $\mathbb{Z}_2^n$ -KD distribution [25]. We now show that there are KD-positive mixed states on 2 qubits that are not mixtures of stabilizer states. Using the techniques from Refs. [23, 25], we construct a state  $\rho_\lambda$  along the di-

rection of some operator  $F$ :

$$\rho_\lambda = \frac{1}{4}I + \lambda F. \quad (16)$$

Informed by the location of the bound states in Fig. 1, we choose  $F$  normal to a facet of both the CSS and rebit-stabilizer polytopes:

$$F = \begin{pmatrix} 1 & 0 & 1 & 1 \\ 0 & 1 & -1 & -1 \\ 1 & -1 & -1 & -2 \\ 1 & -1 & -2 & -1. \end{pmatrix}. \quad (17)$$

Thus, the inner side of the facet can be described by the inequality  $\text{Tr}(\rho F) \leq 1$ . In Supplemental Note V, we show that  $\rho_\lambda$  is a KD-positive state if  $\lambda \in [0, 1/(4 + 8\sqrt{2})]$ . Furthermore, the state  $\rho_\lambda$  lies on the outer side of the facet for  $\lambda > 1/20$  since then  $\text{Tr}(F\rho_\lambda) > 1$ . Thus, for  $\lambda \in ]1/20, 1/(4 + 8\sqrt{2})]$ ,  $\rho_\lambda$  is a 2-qubit bound magic state for the DGBR model. These are not the only bound magic states on 2 qubits: similar bound magic states exist above each of the 20 facets of the CSS polytope that coincides with a facet of the rebit-stabilizer polytope. Using cdd [55], a numerical package for analyzing polytopes, we show this in Supplemental Note V.

The existence of 2-qubit bound magic states implies that bound magic states must also exist for any number of qubits greater than 2. This follows from the fact that partial traces of stabilizer mixtures generate other stabilizer mixtures [56]. Consider the state  $\sigma^{\otimes(n-2)} \otimes \rho_\lambda$ , where  $\sigma$  is some KD-positive single-qubit state and  $\lambda \in ]1/20, 1/(4 + 8\sqrt{2})]$ .  $\sigma^{\otimes(n-2)} \otimes \rho_\lambda$  is KD positive by Theorem 1.4. Moreover,  $\sigma^{\otimes(n-2)} \otimes \rho_\lambda$  cannot be a stabilizer mixture; if it were a stabilizer mixture, then  $\sigma^{\otimes(n-2)} \otimes \rho_\lambda$  after the partial trace over the first  $n-2$  qubits must be a stabilizer mixture, and thus  $\rho_\lambda$  must be a stabilizer mixture, which is not the case. Hence bound states exist for any number of qubits greater than two. Since the convex hull of the KD-positive states is the CSS polytope, and the CSS polytope is a subset of the stabilizer polytope, this also implies that exotic states exist for any number of qubits greater than 2.

To quantify the extent to which the DGBR simulation algorithm differs from the GK simulation algorithm on DGBR circuits, we numerically examine the structure of the 2-qubit state space  $\mathcal{D}((\mathbb{C}^2)^{\otimes 2})$ . Specifically, we compare the (Hilbert-Schmidt) volumes of the regions that the simulation methods can efficiently simulate, as summarized in Table I. Approximately 0.69 % of the states are KD-positive bound states. This increases the known set of simulable states by 15 %. The sampling methodology used in our analysis is detailed in Supplemental Note VI.

*KD Nonpositivity as a Necessary Resource for Quantum Advantage:*—To quantify the resource behind quantum computational advantages, we now bound how much

Category	Simulable by	Proportion
Stabilizer & KD positive	GK&DGBR	1.5614(5) %
Stabilizer & KD nonpositive	GK	2.9753(5) %
Magic & KD positive (bound)	DGBR	0.6868(3) %
Magic & KD nonpositive	Neither	94.7766(6) %

TABLE I. **Estimated Relative Volumes of the Two-Qubit Quantum States.** The relative volumes were estimated by sampling 1 billion random quantum states over the space  $\mathcal{D}((\mathbb{R}^2)^{\otimes 2})$ .

KD nonpositivity is required for arbitrary quantum computations. We construct a monotone for the resource theory of the DGBR model with arbitrary input states. In this resource theory, the free states are the CSS mixtures, and the free operations are those allowed by the DGBR model. We define the KD mana as follows:

$$\mathcal{M}(\rho) := \log \sum_{g, \mathcal{X}} |Q_{g, \mathcal{X}}(\rho)|. \quad (18)$$

**Theorem 2.** *The KD mana satisfies the following properties:*

1. (Faithfulness)  $\mathcal{M}(\rho) = 0$  if and only if  $\rho$  is KD positive.
2. (Additivity) For all density matrices  $\rho$  and  $\sigma$ ,

$$\mathcal{M}(\rho \otimes \sigma) = \mathcal{M}(\rho) + \mathcal{M}(\sigma). \quad (19)$$

3. (Monotone)  $\mathcal{M}$  is nonincreasing under the free operations and is thus a monotone.

Theorem 2.1 follows from the fact that  $\sum_{g, \mathcal{X}} |Q_{g, \mathcal{X}}(\rho)| = 1$  if and only if  $\rho$  is KD positive. The proof of Theorem 2.2 follows from the product rule in Theorem 1.4. Proving Theorem 2.3 amounts to checking that  $\mathcal{M}$  is nonincreasing under the free operations. We give explicit calculations in Supplemental Note VII.

To determine how useful a given state is for quantum computation, one would like to determine if one could map it to another state using free operations. Distillation protocols [1, 3] do exactly that: they take a number of copies of an input state  $\rho$  and map them to a resourceful target state  $\sigma$ . Using an argument analogous to that in Ref. [57], one may use Theorem 2 to lower bound the number of input states required to create a given output state:

**Corollary 1.** *In the DGBR model, any distillation protocol mapping copies of an input state  $\rho$  to a target state  $\sigma$  will require at least  $\mathcal{M}(\sigma)/\mathcal{M}(\rho)$  copies of  $\rho$ .*

This corollary firmly establishes KD nonpositivity as a resource for rebit quantum computation.

*Discussion.*—We have unveiled new methods for examining the DGBR model of quantum computation. We

generalized the rebit-restricted DGBR distribution to an informationally complete  $\mathbb{Z}_2^n$ -KD distribution. Doing so allowed us to repurpose tools developed for the study of the KD distribution to examine the states that when appended to the DGBR model still results in a classically simulable model. Thus, we constructed and analyzed previously unknown bound magic states for the DGBR model, extending the volume of classically simulable input states by 15 %, compared to the GK theorem. Furthermore, we defined the KD mana, related to the nonpositivity of the  $\mathbb{Z}_2^n$ -KD distribution. The KD mana, we showed, is a resource monotone for DGBR computation with arbitrary input states. The KD mana provides an easy-to-calculate bound on the efficiency of distillation protocols. Our work shows that KD nonpositivity is a necessary resource for quantum advantage.

*Acknowledgements.*—JJT was supported by the Cambridge Trust. The authors thank Christopher Long, Joe Smith, Richard Jozsa, Nicole Yunger Halpern, and Ryuji Takagi for helpful discussions. This work was supported in part by the Agence Nationale de la Recherche under grant ANR-11-LABX0007-01 (Labex CEMPI), by the Nord-Pas de Calais Regional Council and the European Regional Development Fund through the Contrat de Projets État-Région (CPER), and by the CNRS through the MITI interdisciplinary programs.

- 
- [1] S. Bravyi and A. Kitaev, Universal quantum computation with ideal clifford gates and noisy ancillas, *Physical Review A* **71**, 10.1103/physreva.71.022316 (2005).
  - [2] S. Aaronson and D. Gottesman, Improved simulation of stabilizer circuits, *Physical Review A* **70**, 10.1103/physreva.70.052328 (2004).
  - [3] B. W. Reichardt, Quantum universality from magic states distillation applied to css codes, *Quantum Information Processing* **4**, 251–264 (2005).
  - [4] E. T. Campbell and D. E. Browne, Bound states for magic state distillation in fault-tolerant quantum computation, *Phys. Rev. Lett.* **104**, 030503 (2010).
  - [5] V. Veitch, C. Ferrie, D. Gross, and J. Emerson, Negative quasi-probability as a resource for quantum computation, *New Journal of Physics* **14**, 113011 (2012).
  - [6] A. Mari and J. Eisert, Positive wigner functions render classical simulation of quantum computation efficient, *Phys. Rev. Lett.* **109**, 230503 (2012).
  - [7] R. Raussendorf, D. E. Browne, N. Delfosse, C. Okay, and J. Bermejo-Vega, Contextuality and wigner-function negativity in qubit quantum computation, *Phys. Rev. A* **95**, 052334 (2017).
  - [8] G. Park, H. Kwon, and H. Jeong, Extending classically simulatable bounds of clifford circuits with nonstabilizer states via framed wigner functions, *Physical Review Letters* **133**, 10.1103/physrevlett.133.220601 (2024).
  - [9] R. Raussendorf, J. Bermejo-Vega, E. Tyhurst, C. Okay, and M. Zurel, Phase-space-simulation method for quantum computation with magic states on qubits, *Phys. Rev.*

- A **101**, 012350 (2020).
- [10] C. Okay, M. Zurel, and R. Raussendorf, On the extremal points of the lambda polytopes and classical simulation of quantum computation with magic states, *Quantum Information and Computation* **21**, 1091–1110 (2021).
- [11] M. Zurel, C. Okay, and R. Raussendorf, Hidden variable model for universal quantum computation with magic states on qubits, *Phys. Rev. Lett.* **125**, 260404 (2020).
- [12] M. Zurel, C. Okay, and R. Raussendorf, Simulating quantum computation: How many “bits” for “it”?, *PRX Quantum* **5**, 10.1103/prxquantum.5.030343 (2024).
- [13] M. Zurel, L. Z. Cohen, and R. Raussendorf, Simulation of quantum computation with magic states via jordan-wigner transformations (2025), arXiv:2307.16034 [quant-ph].
- [14] M. Zurel, L. Z. Cohen, and R. Raussendorf, Simulation of quantum computation with magic states via jordan-wigner transformations (2025), arXiv:2307.16034 [quant-ph].
- [15] M. Zurel and A. Heimendahl, Efficient classical simulation of quantum computation beyond wigner positivity (2024), arXiv:2407.10349 [quant-ph].
- [16] H. Pashayan, J. J. Wallman, and S. D. Bartlett, Estimating outcome probabilities of quantum circuits using quasiprobabilities, *Physical Review Letters* **115**, 10.1103/physrevlett.115.070501 (2015).
- [17] D. Gross, Hudson’s theorem for finite-dimensional quantum systems, *Journal of Mathematical Physics* **47**, 10.1063/1.2393152 (2006).
- [18] N. Delfosse, P. Allard Guerin, J. Bian, and R. Raussendorf, Wigner function negativity and contextuality in quantum computation on rebits, *Phys. Rev. X* **5**, 021003 (2015).
- [19] T. Rudolph and L. Grover, A 2 rebit gate universal for quantum computing (2002), arXiv:quant-ph/0210187 [quant-ph].
- [20] J. G. Kirkwood, Quantum statistics of almost classical assemblies, *Physical Review* **44**, 31 (1933).
- [21] P. A. M. Dirac, On the analogy between classical and quantum mechanics, *Rev. Mod. Phys.* **17**, 195 (1945).
- [22] D. R. M. Arvidsson-Shukur, W. F. Braasch Jr, S. De Bièvre, J. Dressel, A. N. Jordan, C. Langrenez, M. Lostaglio, J. S. Lundeen, and N. Y. Halpern, Properties and applications of the kirkwood–dirac distribution, *New Journal of Physics* **26**, 121201 (2024).
- [23] C. Langrenez, D. R. M. Arvidsson-Shukur, and S. De Bièvre, Characterizing the geometry of the kirkwood–dirac-positive states, *Journal of Mathematical Physics* **65**, 10.1063/5.0164672 (2024).
- [24] C. Langrenez, D. R. M. Arvidsson-Shukur, and S. De Bievre, Convex roofs witnessing kirkwood–dirac nonpositivity, *Journal of Physics A: Mathematical and Theoretical* (2025).
- [25] S. D. Bièvre, C. Langrenez, and D. Radchenko, The kirkwood–dirac representation associated to the fourier transform for finite abelian groups: positivity (2025), arXiv:2501.12252 [quant-ph].
- [26] A. Calderbank, E. Rains, P. Shor, and N. Sloane, Quantum error correction via codes over  $gf(4)$ , *IEEE Transactions on Information Theory* **44**, 1369 (1998).
- [27] A. Steane, Multiple-particle interference and quantum error correction, *Proceedings of the Royal Society of London. Series A: Mathematical, Physical and Engineering Sciences* **452**, 2551–2577 (1996).
- [28] D. Gottesman, Stabilizer codes and quantum error correction (1997), arXiv:quant-ph/9705052 [quant-ph].
- [29] M. A. Nielsen and I. L. Chuang, *Quantum Computation and Quantum Information: 10th Anniversary Edition* (Cambridge University Press, 2010).
- [30] R. Raussendorf and J. Harrington, Fault-tolerant quantum computation with high threshold in two dimensions, *Phys. Rev. Lett.* **98**, 190504 (2007).
- [31] M. Lostaglio, A. Belenchia, A. Levy, S. Hernández-Gómez, N. Fabbri, and S. Gherardini, Kirkwood–Dirac quasiprobability approach to the statistics of incompatible observables, *Quantum* **7**, 1128 (2023).
- [32] D. R. M. Arvidsson-Shukur, N. Yunger Halpern, H. V. Lepage, A. A. Lasek, C. H. W. Barnes, and S. Lloyd, Quantum advantage in postselected metrology, *Nat. Commun.* **11**, 3775 (2020).
- [33] N. Lupu-Gladstein, Y. B. Yilmaz, D. R. M. Arvidsson-Shukur, A. Brodutch, A. O. Pang, A. M. Steinberg, and N. Yunger Halpern, Negative quasiprobabilities enhance phase estimation in quantum-optics experiment, *Physical Review Letters* **128**, 220504 (2022).
- [34] J. H. Jenne and D. R. M. Arvidsson-Shukur, Unbounded and lossless compression of multiparameter quantum information, *Phys. Rev. A* **106**, 042404 (2022).
- [35] Y. Aharonov, D. Z. Albert, and L. Vaidman, How the result of a measurement of a component of the spin of a spin-1/2 particle can turn out to be 100, *Phys. Rev. Lett.* **60**, 1351 (1988).
- [36] J. Dressel, M. Malik, F. M. Miatto, A. N. Jordan, and R. W. Boyd, Colloquium: Understanding quantum weak values: Basics and applications, *Rev. Mod. Phys.* **86**, 307 (2014).
- [37] S. Pang, J. Dressel, and T. A. Brun, Entanglement-assisted weak value amplification, *Phys. Rev. Lett.* **113**, 030401 (2014).
- [38] M. F. Pusey, Anomalous weak values are proofs of contextuality, *Phys. Rev. Lett.* **113**, 200401 (2014).
- [39] J. Dressel, Weak values as interference phenomena, *Phys. Rev. A* **91**, 032116 (2015).
- [40] S. Pang and T. A. Brun, Improving the precision of weak measurements by postselection measurement, *Phys. Rev. Lett.* **115**, 120401 (2015).
- [41] J. J. Thio, W. Salmon, C. H. W. Barnes, S. D. Bièvre, and D. R. M. Arvidsson-Shukur, Contextuality can be verified with noncontextual experiments (2024), arXiv:2412.00199 [quant-ph].
- [42] N. Yunger Halpern, Jarzynski-like equality for the out-of-time-ordered correlator, *Phys. Rev. A* **95**, 012120 (2017).
- [43] M. Lostaglio, Quantum fluctuation theorems, contextuality, and work quasiprobabilities, *Phys. Rev. Lett.* **120**, 040602 (2018).
- [44] M. Lostaglio, Certifying quantum signatures in thermodynamics and metrology via contextuality of quantum linear response, *Phys. Rev. Lett.* **125**, 230603 (2020).
- [45] A. Levy and M. Lostaglio, Quasiprobability distribution for heat fluctuations in the quantum regime, *PRX Quantum* **1**, 010309 (2020).
- [46] M. Lostaglio, A. Belenchia, A. Levy, S. Hernández-Gómez, N. Fabbri, and S. Gherardini, Kirkwood–dirac quasiprobability approach to the statistics of incompatible observables, *Quantum* **7**, 1128 (2023).
- [47] T. Upadhyaya, W. F. Braasch, G. T. Landi, and N. Y. Halpern, Non-abelian transport distinguishes three usually equivalent notions of entropy production, *PRX*

- Quantum **5**, 030355 (2024).
- [48] N. Yunger Halpern, B. Swingle, and J. Dressel, Quasiprobability behind the out-of-time-ordered correlator, *Phys. Rev. A* **97**, 042105 (2018).
- [49] R. Mohseninia, J. R. G. Alonso, and J. Dressel, Optimizing measurement strengths for qubit quasiprobabilities behind out-of-time-ordered correlators, *Phys. Rev. A* **100**, 062336 (2019).
- [50] J. R. González Alonso, N. Yunger Halpern, and J. Dressel, Out-of-time-ordered-correlator quasiprobabilities robustly witness scrambling, *Phys. Rev. Lett.* **122**, 040404 (2019).
- [51] The real part of a KD distribution is sometimes referred to as a Margenau-Hill distribution [58].
- [52] R. Hudson, When is the wigner quasi-probability density non-negative?, *Reports on Mathematical Physics* **6**, 249 (1974).
- [53] E. Wigner, On the quantum correction for thermodynamic equilibrium, *Phys. Rev.* **40**, 749 (1932).
- [54] C. Langrenze, W. Salmon, S. D. Bièvre, J. J. Thio, C. K. Long, and D. R. M. Arvidsson-Shukur, The set of kirkwood-dirac positive states is almost always minimal (2024), arXiv:2405.17557 [quant-ph].
- [55] K. Fukuda, *cdd/cdd+ Reference Manual*, ETH Zurich (1995), available at <https://github.com/cddlib/cddlib>.
- [56] K. M. R. Audenaert and M. B. Plenio, Entanglement on mixed stabilizer states: normal forms and reduction procedures, *New Journal of Physics* **7**, 170–170 (2005).
- [57] V. Veitch, S. A. Hamed Mousavian, D. Gottesman, and J. Emerson, The resource theory of stabilizer quantum computation, *New Journal of Physics* **16**, 013009 (2014).
- [58] H. Margenau and R. N. Hill, Correlation between measurements in quantum theory:, *Progress of Theoretical Physics* **26**, 722 (1961), <https://academic.oup.com/ptp/article-pdf/26/5/722/5454875/26-5-722.pdf>.
- [59] K. Zyczkowski and H.-J. Sommers, Induced measures in the space of mixed quantum states, *Journal of Physics A: Mathematical and General* **34**, 7111 (2001).
-

# Supplemental Material for Kirkwood-Dirac Negativity is a Necessary Resource for Quantum Computing

## I. PROOF OF THE DGBR CONNECTION

We prove Theorem 1.1 of the main article in this Supplemental Note. The phase-space point operators of the  $\mathbb{Z}_2^n$ -KD distribution are

$$B_{\mathbf{g},\boldsymbol{\chi}} = |\boldsymbol{\chi}^{(x)}\rangle \langle \boldsymbol{\chi}^{(x)} | \mathbf{g}^{(z)} \rangle \langle \mathbf{g}^{(z)}|. \quad (\text{S1})$$

We start by showing that the phase-space point operators of the  $\mathbb{Z}_2^n$ -KD distribution may be expressed in terms of the phase-space point operators of the DGBR distribution.

**Lemma S1.** *The phase-space point operators of the DGBR distribution are the hermitianizations of the phase-space point operators of the  $\mathbb{Z}_2^n$ -KD distribution:*

$$A_{\mathbf{g},\boldsymbol{\chi}} = \frac{1}{2}(B_{\mathbf{g},\boldsymbol{\chi}} + B_{\mathbf{g},\boldsymbol{\chi}}^\dagger). \quad (\text{S2})$$

*Proof.* Using that  $A_{\mathbf{g},\boldsymbol{\chi}} = P_{\mathbf{g},\boldsymbol{\chi}} A_{\mathbf{0},\mathbf{0}} P_{\mathbf{g},\boldsymbol{\chi}}^\dagger$ , one may rewrite Eq. (S2) as

$$\frac{1}{2} (P_{\mathbf{g},\boldsymbol{\chi}}^\dagger B_{\mathbf{g},\boldsymbol{\chi}} P_{\mathbf{g},\boldsymbol{\chi}} + (P_{\mathbf{g},\boldsymbol{\chi}}^\dagger B_{\mathbf{g},\boldsymbol{\chi}} P_{\mathbf{g},\boldsymbol{\chi}})^\dagger) = A_{\mathbf{0},\mathbf{0}}. \quad (\text{S3})$$

One may calculate the two terms on the left-hand side to be

$$\begin{aligned} P_{\mathbf{g},\boldsymbol{\chi}}^\dagger B_{\mathbf{g},\boldsymbol{\chi}} P_{\mathbf{g},\boldsymbol{\chi}} &= \prod_{j=1}^n X_j^{g_j} Z_j^{\chi_j} |\boldsymbol{\chi}^{(x)}\rangle \langle \boldsymbol{\chi}^{(x)} | \mathbf{g}^{(z)} \rangle \langle \mathbf{g}^{(z)} | \prod_{k=1}^n Z_k^{\chi_k} X_k^{g_k} \\ &= \langle \boldsymbol{\chi}^{(x)} | \mathbf{g}^{(z)} \rangle (-1)^{\mathbf{x} \cdot \mathbf{g}} |(\boldsymbol{\chi} + \boldsymbol{\chi})^{(x)}\rangle \langle (\mathbf{g} + \mathbf{g})^{(z)}| \\ &= \frac{1}{2^{n/2}} |++ \dots +\rangle \langle 00 \dots 0|, \end{aligned} \quad (\text{S4})$$

where we used that  $X$  and  $Z$  act as boost and shift operators on  $|\mathbf{g}^{(z)}\rangle$  and  $|\boldsymbol{\chi}^{(x)}\rangle$  to go from the first to the second line, and we used that  $\boldsymbol{\chi}$  and  $\mathbf{g}$  are their own inverses to go from the second to the third line. Combining Eqs. (S3) and (S4), we find that the proof amounts to showing that

$$A_{\mathbf{0},\mathbf{0}} = \frac{1}{2 \cdot 2^{n/2}} [ |++ \dots +\rangle \langle 00 \dots 0| + (|++ \dots +\rangle \langle 00 \dots 0|)^\dagger ]. \quad (\text{S5})$$

We show this by expanding  $A_{\mathbf{0},\mathbf{0}}$ :

$$\begin{aligned} A_{\mathbf{0},\mathbf{0}} &= \frac{1}{2^{2n}} \sum_{\substack{\mathbf{g},\boldsymbol{\chi}: \\ \mathbf{g},\boldsymbol{\chi} = \mathbf{0} \pmod{2}}} P_{\mathbf{g},\boldsymbol{\chi}} \\ &= \frac{1}{2 \cdot 2^{2n}} \left( \sum_{\mathbf{g},\boldsymbol{\chi}} P_{\mathbf{g},\boldsymbol{\chi}} + \sum_{\mathbf{g},\boldsymbol{\chi}} (-1)^{\mathbf{g} \cdot \mathbf{x}} P_{\mathbf{g},\boldsymbol{\chi}} \right) \\ &= \frac{1}{2 \cdot 2^{2n}} \left( \sum_{\mathbf{g},\boldsymbol{\chi}} P_{\mathbf{g},\boldsymbol{\chi}} + \left[ \sum_{\mathbf{g},\boldsymbol{\chi}} P_{\mathbf{g},\boldsymbol{\chi}} \right]^\dagger \right) \end{aligned} \quad (\text{S6})$$

Comparing Eqs. (S5) and Eqs. (S6), we find that it suffices to show that

$$\frac{1}{2^{n/2}} |00 \dots 0\rangle \langle ++ \dots +| = \frac{1}{2^{2n}} \sum_{\mathbf{g},\boldsymbol{\chi}} P_{\mathbf{g},\boldsymbol{\chi}}. \quad (\text{S7})$$

We do this by checking the matrix elements of the right-hand side:

$$\begin{aligned}
\frac{1}{2^{2n}} \langle \mathbf{h}^{(z)} | \sum_{\mathbf{g}, \mathbf{x}} P_{\mathbf{g}, \mathbf{x}} | \boldsymbol{\eta}^{(x)} \rangle &= \frac{1}{2^{2n}} \sum_{\mathbf{g}, \mathbf{x}} \langle \mathbf{h}^{(z)} | \prod_j Z_j^{\mathbf{x}_j} X_j^{g_j} | \boldsymbol{\eta}^{(x)} \rangle \\
&= \frac{1}{2^{2n}} \sum_{\mathbf{g}, \mathbf{x}} (-1)^{\mathbf{g} \cdot \mathbf{x}} \langle (\mathbf{g} + \mathbf{h})^{(z)} | (\boldsymbol{\chi} + \boldsymbol{\eta})^{(x)} \rangle \\
&= \frac{(-1)^{\mathbf{h} \cdot \boldsymbol{\eta}}}{2^{n/2} 2^{2n}} \sum_{\mathbf{g}} (-1)^{\mathbf{g} \cdot \boldsymbol{\eta}} \sum_{\mathbf{x}} (-1)^{\mathbf{h} \cdot \mathbf{x}} \\
&= \frac{1}{2^{n/2}} \delta_{\mathbf{h}, \mathbf{0}} \delta_{\boldsymbol{\eta}, \mathbf{0}}, \tag{S8}
\end{aligned}$$

where we used the properties of  $X$  and  $Z$  as boost and shift operators to go from the first to the second line, the fact that  $\langle \mathbf{g}^{(z)} | \boldsymbol{\chi}^{(x)} \rangle = (-1)^{\mathbf{g} \cdot \mathbf{x}} / 2^{n/2}$  to go from the second to the third line, and the fact that  $\sum_{\mathbf{g}} (-1)^{\mathbf{g} \cdot \boldsymbol{\eta}} = 2^n \delta_{\boldsymbol{\eta}, \mathbf{0}}$  to go from the third to the fourth line. Eq. (S8) establishes Eq. (S7), completing the proof.  $\square$

We now use this lemma to prove Theorem 1.1.

**Lemma S2** (DGBR Connection). *Let  $W_{\mathbf{g}, \mathbf{x}}$  and  $Q_{\mathbf{g}, \mathbf{x}}$  denote the DGBR distribution and the  $\mathbb{Z}_2^n$ -KD distribution respectively. Then  $\text{Re}[Q_{\mathbf{g}, \mathbf{x}}(\rho)] = W_{\mathbf{g}, \mathbf{x}}(\rho)$ .*

*Proof.* Substituting Eq. (S2) into Eq. (2) of the main article and evaluating the trace in the computational basis yields

$$\begin{aligned}
W_{\mathbf{g}, \mathbf{x}}(\rho) &= \text{Tr} \left[ \frac{1}{2} (B_{\mathbf{g}, \mathbf{x}} + B_{\mathbf{g}, \mathbf{x}}^\dagger) \rho \right] \\
&= \frac{1}{2} \sum_{\mathbf{h}, \mathbf{h}'} \langle \mathbf{h}^{(z)} | B_{\mathbf{g}, \mathbf{x}} | \mathbf{h}'^{(z)} \rangle \text{Re} \left( \langle \mathbf{h}'^{(z)} | \rho | \mathbf{h}^{(z)} \rangle \right) + \frac{1}{2} i \sum_{\mathbf{h}, \mathbf{h}'} \langle \mathbf{h}^{(z)} | B_{\mathbf{g}, \mathbf{x}} | \mathbf{h}'^{(z)} \rangle \text{Im} \left( \langle \mathbf{h}'^{(z)} | \rho | \mathbf{h}^{(z)} \rangle \right) \\
&\quad + \frac{1}{2} \sum_{\mathbf{h}, \mathbf{h}'} \langle \mathbf{h}'^{(z)} | B_{\mathbf{g}, \mathbf{x}} | \mathbf{h}^{(z)} \rangle \text{Re} \left( \langle \mathbf{h}'^{(z)} | \rho | \mathbf{h}^{(z)} \rangle \right) + \frac{1}{2} i \sum_{\mathbf{h}, \mathbf{h}'} \langle \mathbf{h}'^{(z)} | B_{\mathbf{g}, \mathbf{x}} | \mathbf{h}^{(z)} \rangle \text{Im} \left( \langle \mathbf{h}'^{(z)} | \rho | \mathbf{h}^{(z)} \rangle \right) \tag{S9}
\end{aligned}$$

where we used that the matrix elements of the phase-space point operators of the  $\mathbb{Z}_2^n$ -KD distribution are real in the computational basis. Reindexing the third and fourth sum and using that the real and imaginary parts of  $\rho$  are symmetric and anti-symmetric respectively, we find that

$$\begin{aligned}
W_{\mathbf{g}, \mathbf{x}}(\rho) &= \frac{1}{2} \sum_{\mathbf{h}, \mathbf{h}'} \langle \mathbf{h}^{(z)} | B_{\mathbf{g}, \mathbf{x}} | \mathbf{h}'^{(z)} \rangle \text{Re} \left( \langle \mathbf{h}'^{(z)} | \rho | \mathbf{h}^{(z)} \rangle \right) + \frac{1}{2} i \sum_{\mathbf{h}, \mathbf{h}'} \langle \mathbf{h}^{(z)} | B_{\mathbf{g}, \mathbf{x}} | \mathbf{h}'^{(z)} \rangle \text{Im} \left( \langle \mathbf{h}'^{(z)} | \rho | \mathbf{h}^{(z)} \rangle \right) \\
&\quad + \frac{1}{2} \sum_{\mathbf{h}, \mathbf{h}'} \langle \mathbf{h}^{(z)} | B_{\mathbf{g}, \mathbf{x}} | \mathbf{h}'^{(z)} \rangle \text{Re} \left( \langle \mathbf{h}'^{(z)} | \rho | \mathbf{h}^{(z)} \rangle \right) - \frac{1}{2} i \sum_{\mathbf{h}, \mathbf{h}'} \langle \mathbf{h}^{(z)} | B_{\mathbf{g}, \mathbf{x}} | \mathbf{h}'^{(z)} \rangle \text{Im} \left( \langle \mathbf{h}'^{(z)} | \rho | \mathbf{h}^{(z)} \rangle \right) \\
&= \text{Re} \sum_{\mathbf{h}, \mathbf{h}'} \langle \mathbf{h}^{(z)} | B_{\mathbf{g}, \mathbf{x}} | \mathbf{h}'^{(z)} \rangle \text{Re} \left( \langle \mathbf{h}'^{(z)} | \rho | \mathbf{h}^{(z)} \rangle \right) \\
&= \text{Re} \text{Tr}(B_{\mathbf{g}, \mathbf{x}} \rho) \\
&= \text{Re}[Q_{\mathbf{g}, \mathbf{x}}(\rho)] \tag{S10}
\end{aligned}$$

$\square$

## II. PROOF OF HUDSON'S THEOREM FOR THE $\mathbb{Z}_2^n$ -KD DISTRIBUTION

We prove Theorem 1.2 of the main article in this Supplemental Note.

**Lemma S3** (Hudson's Theorem for the  $\mathbb{Z}_2^n$ -KD Distribution). *Let  $|\psi\rangle \in \mathcal{H}$ .  $|\psi\rangle$  is KD positive if and only if  $|\psi\rangle$  is a CSS state.*

*Proof.* In [25], it was shown that for a KD distribution based on the group  $G$ ,  $|\psi\rangle$  is KD positive if and only if it is of the form

$$|H; \mathbf{g}, \boldsymbol{\chi}\rangle := \frac{1}{|H|^{1/2}} P_{\mathbf{g}, \boldsymbol{\chi}} \sum_{\mathbf{h} \in H} |\mathbf{h}^{(z)}\rangle := P_{\mathbf{g}, \boldsymbol{\chi}} |H\rangle, \quad (\text{S11})$$

where  $H$  is a subgroup of  $G$ . We are thus left to show that (i)  $|H; \mathbf{g}, \boldsymbol{\chi}\rangle$  is a CSS state, and that (ii) all CSS states are of the form  $|H; \mathbf{g}, \boldsymbol{\chi}\rangle$ .

We start with (i). To determine if  $|H; \mathbf{g}, \boldsymbol{\chi}\rangle$  is a CSS state, we need to find its maximal stabilizing subgroup. We first focus on  $|H\rangle$ . Let  $H^\perp$  denote the set of characters in  $\hat{G}$  that are trivial on  $H$ . That is  $H^\perp := \{\boldsymbol{\chi} \in \hat{G} | \boldsymbol{\chi}(\mathbf{h}) = 1 \forall \mathbf{h} \in H\}$ . We consider the following subgroup of the Pauli group:

$$\langle \{P_{\mathbf{h}, \mathbf{0}}\}_{\mathbf{h} \in H} \cup \{P_{\mathbf{0}, \boldsymbol{\eta}}\}_{\boldsymbol{\eta} \in H^\perp} \rangle = \{P_{\mathbf{h}, \boldsymbol{\eta}} | \mathbf{h} \in H, \boldsymbol{\eta} \in H^\perp\}. \quad (\text{S12})$$

Since  $H$  is closed under group addition and since group addition is an isomorphism, we find that  $P_{\mathbf{h}, \mathbf{0}} |H\rangle = |H + \mathbf{h}\rangle = |H\rangle$ . Furthermore, since  $\boldsymbol{\eta} \in H^\perp$ , we also find that  $P_{\mathbf{0}, \boldsymbol{\eta}} |H\rangle = |\boldsymbol{\eta}(H)\rangle = |H\rangle$ . Hence Eq. (S12) is a stabilizing subgroup. To show that this stabilizing subgroup indeed uniquely determines  $|H\rangle$ , we must show that it is maximal in the sense that its size is  $2^n$  [2].

In view of Eq. (S12), there are  $|H| \times |H^\perp|$  distinct stabilizers. We must therefore show that  $|H| \times |H^\perp| = 2^n$ .

To this end, we consider the group homomorphism  $\phi: \hat{G} \rightarrow \hat{H}$  defined by the restriction map  $\boldsymbol{\chi} \mapsto \boldsymbol{\chi}|_H$ , where  $\hat{H}$  is the character group of  $H$ . Clearly,  $\ker \phi = H^\perp$  and  $\text{ran } \phi = \hat{H}$ , where  $\text{ran}$  denotes the range (image) of a function. The first isomorphism theorem then implies that

$$\hat{G}/H^\perp = \hat{G}/\ker \phi \cong \text{ran } \phi = \hat{H} \cong H \quad (\text{S13})$$

from which it follows that  $|H| \times |H^\perp| = |G| = 2^n$ . The stabilizing subgroup Eq. (S12) is therefore maximal and thus uniquely defines  $|H\rangle$ .

To characterize the stabilizing subgroup of  $|H; \mathbf{g}, \boldsymbol{\chi}\rangle$ , note that if  $S$  stabilizes  $|\psi\rangle$ , then  $P_{\mathbf{g}, \boldsymbol{\chi}} S P_{\mathbf{g}, \boldsymbol{\chi}}^\dagger$  stabilizes  $P_{\mathbf{g}, \boldsymbol{\chi}} |\psi\rangle$ . The maximal stabilizing subgroup for  $|H; \mathbf{g}, \boldsymbol{\chi}\rangle$  is therefore

$$\langle \{(-1)^{\mathbf{h} \cdot \boldsymbol{\chi}} P_{\mathbf{h}, \mathbf{0}}\}_{\mathbf{h} \in H} \cup \{(-1)^{\mathbf{g} \cdot \boldsymbol{\eta}} P_{\mathbf{0}, \boldsymbol{\eta}}\}_{\boldsymbol{\eta} \in H^\perp} \rangle, \quad (\text{S14})$$

where we used that  $P_{\mathbf{g}, \boldsymbol{\chi}} P_{\mathbf{h}, \boldsymbol{\eta}} = (-1)^{\mathbf{g} \cdot \boldsymbol{\eta} + \mathbf{h} \cdot \boldsymbol{\chi}} P_{\mathbf{h}, \boldsymbol{\eta}} P_{\mathbf{g}, \boldsymbol{\chi}}$  and that  $P_{\mathbf{g}, \boldsymbol{\chi}} P_{\mathbf{g}, \boldsymbol{\chi}}^\dagger = I$ . The stabilizing subgroup of  $|H; \mathbf{g}, \boldsymbol{\chi}\rangle$  therefore is of the form  $\langle U \cup V \rangle$ , where  $U$  and  $V$  are sets containing Pauli operators with only  $Z$ s and  $X$ s respectively. Hence  $|H; \mathbf{g}, \boldsymbol{\chi}\rangle$  is a CSS state.

We move on to proving the converse statement (ii). If  $|\psi\rangle$  is a CSS state, then it has a stabilizing subgroup of the form  $\langle S_Z \cup S_X \rangle$ , where we may take  $S_Z$  and  $S_X$  to be subgroups of the Pauli group of the form  $S_Z = \{(-1)^{f(\mathbf{h})} P_{\mathbf{h}, \mathbf{0}}\}_{\mathbf{h} \in H}$  and  $S_X = \{(-1)^{g(\boldsymbol{\eta})} P_{\mathbf{0}, \boldsymbol{\eta}}\}_{\boldsymbol{\eta} \in K}$ , where  $f$  and  $g$  are binary functions and  $H$  and  $K$  are subsets of  $G, \hat{G}$  respectively [26–28]. To show that this maximal stabilizing subgroup corresponds to a state of the form  $|H; \mathbf{g}, \boldsymbol{\chi}\rangle$ , we must show that it can be written in the form (S14). That is, we need to show that  $H$  is a subgroup of  $G$ ; that  $K = H^\perp$ ; and that there exist  $\mathbf{g}, \boldsymbol{\chi} \in G, \hat{G}$  such that  $f(\mathbf{h}) = \boldsymbol{\chi} \cdot \mathbf{h}$  and  $g(\boldsymbol{\eta}) = \mathbf{g} \cdot \boldsymbol{\eta}$ .

We start by showing that the subset  $H$  is a subgroup of  $G$ . To do this, we must show that  $H$  is closed under group addition and inversion and that  $H$  must contain the identity. Suppose  $\mathbf{h}, \mathbf{h}' \in H$ , then

$$(-1)^{f(\mathbf{h})} P_{\mathbf{h}, \mathbf{0}} (-1)^{f(\mathbf{h}')} P_{\mathbf{h}', \mathbf{0}} = (-1)^{f(\mathbf{h}) + f(\mathbf{h}')} P_{\mathbf{h} + \mathbf{h}', \mathbf{0}} \in S_Z. \quad (\text{S15})$$

Hence,  $\mathbf{h} + \mathbf{h}' \in H$ , and closure under group addition follows. Furthermore, note that  $\forall \mathbf{h} \in H, -\mathbf{h} = \mathbf{h}$  since  $H$  is a subset of  $G = \mathbb{Z}_2^n$ . Hence,  $H$  is also closed under inversion. Last, since  $H$  is closed under group addition and  $\mathbf{h} + \mathbf{h} = \mathbf{0}$ , we have that  $H$  also contains the identity. Hence,  $H$  is a subgroup of  $G$ . Similar arguments show that  $K$  is a subgroup of  $\hat{G}$ .

Next, we prove that  $K = H^\perp$ . Let  $\mathbf{k} \in K$ . Note that since  $\langle S_Z \cup S_X \rangle$  is a stabilizing subgroup, all its elements must commute. Hence,  $\forall \mathbf{h} \in H, P_{\mathbf{k}, \mathbf{0}} P_{\mathbf{h}, \mathbf{0}} = P_{\mathbf{h}, \mathbf{0}} P_{\mathbf{k}, \mathbf{0}}$ . But from the Pauli commutation relationships, we also know that  $P_{\mathbf{k}, \mathbf{0}} P_{\mathbf{h}, \mathbf{0}} = (-1)^{\mathbf{k} \cdot \mathbf{h}} P_{\mathbf{h}, \mathbf{0}} P_{\mathbf{k}, \mathbf{0}}$ . This implies that  $\forall \mathbf{h} \in H, \mathbf{k}(\mathbf{h}) = (-1)^{\mathbf{k} \cdot \mathbf{h}} = 1$ . Hence,  $\mathbf{k} \in H^\perp$  and thus  $K \subset H^\perp$ . Furthermore, since  $\langle S_Z \cup S_X \rangle$  is a maximal stabilizing subgroup, we must have that  $|K| = |H^\perp|$ . It follows that  $K = H^\perp$ .

Last, we must show that there exist  $\mathbf{g}, \boldsymbol{\chi} \in G, \hat{G}$  such that  $f(\mathbf{h}) = \boldsymbol{\chi} \cdot \mathbf{h}$  and  $g(\boldsymbol{\eta}) = \mathbf{g} \cdot \boldsymbol{\eta}$ . From Eq. (S15), it follows that  $f(\mathbf{h}) + f(\mathbf{h}') = f(\mathbf{h} + \mathbf{h}')$ , i.e.  $f$  is a linear map from  $H$  to the set  $\{0, 1\}$ . It follows that there must exist a  $\boldsymbol{\chi} \in \hat{G}$  such that  $f(\mathbf{h}) = \boldsymbol{\chi} \cdot \mathbf{h}$ . The same argument also applies to  $g$ . We have thus shown that all CSS states are of the form  $|H; \mathbf{g}, \boldsymbol{\chi}\rangle$ , completing the proof.  $\square$

### III. PROOF OF THE COVARIANCE RELATIONSHIPS

We prove Theorem 1.3 of the main article in this Supplemental Note.

**Lemma S4** (Covariance). *The  $\mathbb{Z}_2^n$ -KD distribution obeys the following covariance relationships:*

$$Q_{g_0, \chi_0}(P_{g, \chi} \rho P_{g, \chi}^\dagger) = Q_{g_0 + g, \chi_0 + \chi}(\rho) \quad (\text{S16})$$

$$Q_{g, \chi}(\mathbb{H}^{\otimes n} \rho \mathbb{H}^{\otimes n \dagger}) = \overline{Q_{\chi, g}(\rho)} \quad (\text{S17})$$

$$Q_{g, \chi}(\text{CNOT}_{ct} \rho \text{CNOT}_{ct}^\dagger) = Q_{A_{ct}g, B_{ct}\chi}(\rho), \quad (\text{S18})$$

where  $(A_{ct})_{jk} := \delta_{jk} + \delta_{tj}\delta_{ck}$  and  $(B_{ct})_{jk} := \delta_{jk} + \delta_{cj}\delta_{tk}$ .

*Proof.* Covariance relation (S16) follows directly from Eq. (29) in [25]. We move on to showing covariance relation (S17). The effect of the simultaneous Hadamard on such states is  $\mathbb{H}^{\otimes n} |\mathbf{a}^{(x)}\rangle = |\mathbf{a}^{(z)}\rangle$ . We thus find that

$$\begin{aligned} Q_{g, \chi}(\mathbb{H}^{\otimes n} \rho \mathbb{H}^{\otimes n \dagger}) &= \langle \chi^{(x)} | \mathbb{H}^{\otimes n} \mathbb{H}^{\otimes n} |g^{(z)}\rangle \langle g^{(z)} | \mathbb{H}^{\otimes n} \rho \mathbb{H}^{\otimes n} | \chi^{(x)} \rangle \\ &= \langle \chi^{(z)} |g^{(x)}\rangle \langle g^{(x)} | \rho | \chi^{(z)} \rangle \\ &= \overline{\langle g^{(x)} | \chi^{(z)} \rangle \langle \chi^{(z)} | \rho | g^{(x)} \rangle} \\ &= \overline{Q_{\chi, g}(\rho)}, \end{aligned} \quad (\text{S19})$$

proving the result. Finally we prove covariance relation (S18). To do this, we use that  $\text{CNOT} |a^{(z)}\rangle \otimes |b^{(z)}\rangle = |a^{(z)}\rangle \otimes |(a+b)^{(z)}\rangle$  and that  $\text{CNOT} |a^{(x)}\rangle \otimes |b^{(x)}\rangle = |(a+b)^{(x)}\rangle \otimes |b^{(x)}\rangle$ . This implies that  $\text{CNOT}_{ct} |g^{(z)}\rangle = |A_{ct}g^{(z)}\rangle$  and  $\text{CNOT}_{ct} | \chi^{(x)} \rangle = |B_{ct}\chi^{(x)}\rangle$ , where  $(A_{ct})_{jk} := \delta_{jk} + \delta_{tj}\delta_{ck}$  and  $(B_{ct})_{jk} := \delta_{jk} + \delta_{cj}\delta_{tk}$ . We thus find that

$$\begin{aligned} Q_{g, \chi}(\text{CNOT}_{ct} \rho \text{CNOT}_{ct}^\dagger) &= \langle \chi^{(x)} | \text{CNOT}_{ct} \text{CNOT}_{ct} |g^{(z)}\rangle \langle g^{(z)} | \text{CNOT}_{ct} \rho \text{CNOT}_{ct} | \chi^{(x)} \rangle \\ &= \langle B_{ct}\chi^{(x)} | A_{ct}g^{(z)} \rangle \langle A_{ct}g^{(z)} | \rho | B_{ct}\chi^{(x)} \rangle \\ &= Q_{A_{ct}g, B_{ct}\chi} \end{aligned} \quad (\text{S20})$$

establishing the last covariance relation.  $\square$

### IV. KD-BASED SIMULATION ALGORITHM

It was shown in the main article that KD-positive input states may be efficiently simulated using the simulation algorithm built on the DGBR distribution from Ref. [18]. We now show that the DGBR simulation algorithm may be phrased entirely in terms of the  $\mathbb{Z}_2^n$ -KD distribution.

---

#### Algorithm 1 Phase-Space Simulation Algorithm

---

**Input:** DGBR circuit  $C$  and KD-positive input state  $\rho_{\text{input}}$

**Output:** bitstring  $(b_j)_j$

- 1: Sample  $g, \chi$  from  $Q(\rho_{\text{input}})$
  - 2: **for** each gate in circuit  $C$  **do**
  - 3:     **If** the gate is  $P_{g', \chi'}$ , set  $g \leftarrow g + g'$  and  $\chi \leftarrow \chi + \chi'$
  - 4:     **If** the gate is  $\mathbb{H}$ , set  $g, \chi \leftarrow \chi, g$
  - 5:     **If** the gate is  $\text{CNOT}_{ct}$ , set  $g \leftarrow A_{ct}g$  and  $\chi \leftarrow B_{ct}\chi$
  - 6:     **If** the gate is a  $Z$ -measurement of the  $j$ th qubit:
  - 7:         Output the bit  $b = g_j$
  - 8:         With probability  $1/2$ , set  $\chi \leftarrow \chi + \mathbf{e}_j$ .
  - 9: **end for**
- 

In the above,  $\mathbf{e}_j$  is the vector with a 1 in the  $j$ th entry and zero elsewhere, and  $A_{ct}$  and  $B_{ct}$  are defined in the main article.. This algorithm runs in linear time. To prove its correctness, we need the following lemma:

**Lemma S5.** *If the  $j$ th qubit of a state  $\rho$  is measured in the computational basis and we find output  $b = g_j$ , then the  $\mathbb{Z}_2^n$ -KD distribution of the updated state  $\rho'$  is*

$$Q_{g, \chi}(\rho') = \frac{1}{2} [Q_{g, \chi}(\rho) + Q_{g, \chi + \mathbf{e}_j}(\rho)]. \quad (\text{S21})$$

*Proof.* After the measurement, the state is updated to

$$\begin{aligned}\rho' &\propto [I + (-1)^b Z_j] \rho [I + (-1)^b Z_j] \\ &= \rho + (-1)^b Z_j \rho + (-1)^b \rho Z_j + Z_j \rho Z_j.\end{aligned}\tag{S22}$$

One may straightforwardly calculate that

$$Q_{\mathbf{g}, \boldsymbol{\chi}}(Z_j \rho) = (-1)^{g_j} Q_{\mathbf{g}, \boldsymbol{\chi}}(\rho),\tag{S23}$$

and

$$Q_{\mathbf{g}, \boldsymbol{\chi}}(\rho Z_j) = (-1)^{g_j} Q_{\mathbf{g}, \boldsymbol{\chi} + \mathbf{e}_j}(\rho).\tag{S24}$$

Taking the KD-distribution of Eq. (S22), and substituting in Eqs. (S23) and (S24) together with covariance relation (S16) then yields:

$$Q_{\mathbf{g}, \boldsymbol{\chi}}(\rho') \propto Q_{\mathbf{g}, \boldsymbol{\chi}}(\rho) + Q_{\mathbf{g}, \boldsymbol{\chi} + \mathbf{e}_j}(\rho).\tag{S25}$$

Normalization yields the desired result.  $\square$

We now prove the correctness of our simulation algorithm:

**Theorem S6.** *Let  $C$  be a DGBR circuit with input state  $\rho$ . If  $\rho$  is KD positive and we can sample efficiently from  $Q(\rho)$ , then there exists an efficient classical algorithm that samples from the same probability distribution as the quantum circuit.*

*Proof.* We prove this by showing that Algorithm 1 samples from the correct output distribution. We will use an approach similar to the one taken for the proof of Theorem 1 in Ref. [5]. Let  $\rho_p$  denote the state of the qubits after the  $p$ th gate is applied. We first show by induction that after  $p$  steps,  $\mathbf{g}$  and  $\boldsymbol{\chi}$  are distributed according to  $Q(\rho_p)$ . This is trivially true for  $p = 0$ , establishing the base case. Assume it is true for  $p$ . If we apply a Pauli gate  $P_{\mathbf{g}_0, \boldsymbol{\chi}_0}$  at time step  $p$ , then  $Q_{\mathbf{g}, \boldsymbol{\chi}}(\rho_{p+1}) = Q_{\mathbf{g}, \boldsymbol{\chi}}(P_{\mathbf{g}, \boldsymbol{\chi}} \rho_p P_{\mathbf{g}_0, \boldsymbol{\chi}_0}^\dagger) = Q_{\mathbf{g} + \mathbf{g}_0, \boldsymbol{\chi} + \boldsymbol{\chi}_0}(\rho_p)$ , where we used covariance relationship (S16) in the second equality. It follows that updating  $\mathbf{g}$  to  $\mathbf{g} + \mathbf{g}_0$  and  $\boldsymbol{\chi}$  to  $\boldsymbol{\chi} + \boldsymbol{\chi}_0$  ensures that  $\mathbf{g}$  and  $\boldsymbol{\chi}$  are distributed according to  $Q_{\mathbf{g}, \boldsymbol{\chi}}(\rho_{p+1})$ . Similar arguments apply to when  $H^{\otimes n}$  or  $\text{CNOT}_{ct}$  are applied.

If a measurement is applied at timestep  $t$ , then we obtain the outcome  $b = g$ . Using Lemma S5, we know that  $Q_{\mathbf{g}, \boldsymbol{\chi}}(\rho_{p+1})$  is distributed according to  $\frac{1}{2} [Q_{\mathbf{g}, \boldsymbol{\chi}}(\rho_p) + Q_{\mathbf{g}, \boldsymbol{\chi} + \mathbf{e}_j}(\rho_p)]$ . Thus updating  $\boldsymbol{\chi}$  to  $\boldsymbol{\chi} + \mathbf{e}_j$  with a probability 1/2 indeed ensures that  $\mathbf{g}$  and  $\boldsymbol{\chi}$  are distributed according to  $Q_{\mathbf{g}, \boldsymbol{\chi}}(\rho_{p+1})$ . This completes the proof by induction.

We are left to show that given a state  $\rho_p$ , measuring the  $j$ th qubit in the computational basis is indeed the same as sampling  $\mathbf{g}, \boldsymbol{\chi}$  from  $Q(\rho)$  and returning  $g_j$ . The probability of getting outcome  $b$  when measuring qubit  $j$  is

$$\begin{aligned}\mathbb{P}(Z_j = b | \rho_p) &= \text{Tr} \left[ \frac{1}{2} (1 + (-1)^b Z_j) \rho_p \right] \\ &= \sum_{\mathbf{g}, \boldsymbol{\chi}} \tilde{Q}_{\mathbf{g}, \boldsymbol{\chi}} \left( \frac{1}{2} (1 + (-1)^b Z_j) \right) Q_{\mathbf{g}, \boldsymbol{\chi}}(\rho_p),\end{aligned}\tag{S26}$$

where the overlap formula (Eq. (8) of the main article) was used. A straightforward calculation shows that

$$\begin{aligned}\tilde{Q}_{\mathbf{g}, \boldsymbol{\chi}} \left( \frac{1}{2} (1 + (-1)^b Z_j) \right) &= \frac{\langle \chi_j^{(x)} | I + (-1)^b Z | g_j^{(z)} \rangle}{\langle \chi_j^{(x)} | g_j^{(z)} \rangle} \\ &= \delta_{g_j, b}.\end{aligned}\tag{S27}$$

We thus find that

$$\mathbb{P}(Z_j = b | \rho_p) = \sum_{\mathbf{g}, \boldsymbol{\chi}: g_j = b} Q_{\mathbf{g}, \boldsymbol{\chi}}(\rho_p).\tag{S28}$$

*Id est*, the probability of obtaining outcome  $b$  is equal to sampling outcome  $\mathbf{g}, \boldsymbol{\chi}$  from  $Q(\rho)$  and obtaining  $g_j = b$ .  $\square$

## V. ANALYTICAL CONSTRUCTION OF BOUND STATES

In the main article, we considered an operator  $F$  normal to a facet of both the CSS and rebit stabilizer polytopes:

$$F = \begin{pmatrix} 1 & 0 & 1 & 1 \\ 0 & 1 & -1 & -1 \\ 1 & -1 & -1 & -2 \\ 1 & -1 & -2 & -1. \end{pmatrix}. \quad (\text{S29})$$

The half-space corresponding to this facet is defined by the inequality  $\text{Tr}(\rho F) \leq 1$ . For all 24 rebit stabilizer states on 2 qubits and for all 20 CSS states on 2 qubits,  $\text{Tr}(\rho F) \leq 1$ . The inequality is tight for at least 9 states in each case. Since the dimensionality of the affine space the rebit states live in is 9, this means that  $\text{Tr}(\rho F) \leq 1$  indeed defines a facet of both polytopes.

We considered the state  $\rho_\lambda$ , given by

$$\rho_\lambda = \frac{1}{4}I + \lambda F, \quad (\text{S30})$$

and noted that this state lies outside the rebit stabilizer polytope for  $\lambda > 1/20$ . Since the rebit stabilizer polytope contains all real stabilizer mixtures, and since  $\rho_\lambda$  is real for all  $\lambda$ , this implies that  $\rho_\lambda$  is magic for  $\lambda > 1/20$ .

Finally, to show that  $\rho_\lambda$  is a bound magic state, we must find the  $\lambda$  for which  $\rho_\lambda$  is a KD-positive state. We start with KD-positivity. The KD-distribution of  $\rho_\lambda$  is given by

$$Q(\rho_\lambda) = \frac{1}{15} \begin{pmatrix} 1+12\lambda & 1+4\lambda & 1-4\lambda & 1+4\lambda \\ 1-4\lambda & 1+4\lambda & 1+12\lambda & 1+4\lambda \\ 1-12\lambda & 1+12\lambda & 1-12\lambda & 1-4\lambda \\ 1-12\lambda & 1-4\lambda & 1-12\lambda & 1+12\lambda \end{pmatrix}. \quad (\text{S31})$$

$\rho_\lambda$  therefore is a KD positive operator for  $\lambda \in [-1/12, 1/12]$ .

Next, we need to find the values of  $\lambda$  for which  $\rho_\lambda$  is indeed a quantum state. By construction,  $\rho_\lambda$  is Hermitian and trace 1 for all  $\lambda$ , so for  $\rho_\lambda$  to be a quantum state, we only need to ensure that it is positive semidefinite. We may ensure positive semidefiniteness by requiring all the eigenvalues of  $\rho_\lambda$  to be nonnegative. Letting  $\mu_j$  denote the eigenvalues of  $\rho_\lambda$ , the characteristic equation shows that

$$\det(\lambda F - (\mu_j - 1/4)I) = 0. \quad (\text{S32})$$

Denoting the eigenvalues of  $F$  by  $\nu_j$ , we thus find that

$$\mu_j = \lambda \nu_j + 1/4. \quad (\text{S33})$$

The minimal eigenvalue of  $F$  may be calculated to be  $-1 - 2\sqrt{2}$  using standard methods. Using Eq. (S33), we find that  $\rho_\lambda$  is positive semidefinite and thus a state for  $\lambda \in [0, 1/(4 + 8\sqrt{2})]$ . This is a stronger requirement than KD-positivity, so we find that  $\rho_\lambda$  is a KD positive state for  $\lambda \in [0, 1/(4 + 8\sqrt{2})]$ .

Putting these results together, we find that  $\rho_\lambda$  is both magic and a KD-positive state for  $\lambda \in [1/20, 1/(4 + 8\sqrt{2})]$ . Since KD-positive states are simulable,  $\rho_\lambda$  must therefore be a bound magic state for  $\lambda \in [1/20, 1/(4 + 8\sqrt{2})]$ .

## VI. NUMERICAL CONSTRUCTION OF BOUND STATES ABOVE CSS FACETS

In this Supplemental Note, we numerically show that there exist bound states above every facet shared between the CSS and rebit stabilizer polytope. To do this, we first need an explicit description of the rebit stabilizer and CSS polytopes. We may express any 2-qubit state  $\rho$  in the Pauli basis using

$$\rho = \sum_{P_1, P_2 \in \{I, X, Y, Z\}} r_{P_1, P_2}(\rho) P_1 \otimes P_2, \quad (\text{S34})$$

where  $r_{P_1, P_2}(\rho)$  are the coordinates of  $\rho$  in this basis. Note that  $r_{P_1, P_2}(\rho)$  must be real and that  $r_{I, I}(\rho) = 1/4$ . This means that the coordinates of the stabilizer states live in an affine subspace of  $\mathbb{R}^{16}$ .

To find all the facets of the rebit stabilizer and CSS polytopes, we express the rebit stabilizer and CSS states in the Pauli basis. There are 24 2-qubit rebit stabilizer states, of which 20 are CSS. We thus get 24 points in  $\mathbb{R}^{16}$ , of which 20 belong to CSS states. We use cdd [55], a numerical package for analyzing polytopes in  $\mathbb{R}^m$ , to find the facets of these polytopes. We find that the rebit stabilizer polytope has 120 facets and the CSS polytope has 40 facets. Between these two sets of facets, exactly 24 facets coincide.

We take the normal of each shared facet  $F$  and consider a state  $\rho_\lambda = I/4 + \lambda F$  along this normal as in Note V. Using a bisection method, we numerically find  $\lambda_{\text{KD}+}$ , the maximal  $\lambda$  for which  $\rho_\lambda$  is KD positive. Similarly, we also numerically find  $\lambda_{\text{SD}}$ , the largest value of  $\lambda$  for which  $\rho_\lambda$  only has positive eigenvalues and thus is a valid density matrix.

To determine whether a state is magic, we consider the following linear program:

$$\begin{aligned} \max_{p_S} 0 \quad \text{s.t.} \quad & \sum_S p_S S = \rho_\lambda, \\ & \text{and } \sum_S p_S = 1, \\ & \text{and } p_S \geq 0, \end{aligned} \tag{S35}$$

where the sums are taken over all 2-qubit stabilizer states. If this linear program is feasible, then  $\rho_\lambda$  must be a stabilizer mixture. If the linear program is infeasible, then  $\rho_\lambda$  must be magic. Using a bisection method with a linear program solver as a subroutine, we numerically find  $\lambda_{\text{magic}}$ , the largest value of  $\lambda$  for which  $\rho_\lambda$  is a stabilizer mixture.

For every shared facet, we find  $\lambda_{\text{KD}+} = 0.083$ ,  $\lambda_{\text{SD}} = 0.065$  and  $\lambda_{\text{magic}} = 0.050$ . These values agree up to numerical precision with those obtained using the analytical approach in Note V. Since  $\lambda_{\text{magic}} \leq \lambda_{\text{KD}+}$  and  $\lambda_{\text{magic}} \leq \lambda_{\text{SD}}$ , we have found bound states above every shared facet of the stabilizer polytope.

## VII. ESTIMATION OF RELATIVE VOLUME OF BOUND STATES

In this Supplemental Note, we describe our methodology for obtaining the data presented in Table I of the main article. We aim to estimate the relative volumes that the four simulation categories occupy in the two-qubit rebit state space. Here, the volume is estimated by the ratio of the number of random samples falling into a given category to the total number of sampled states.

To ensure unbiased sampling, we generate random rebit density matrices using the real Ginibre ensemble. This construction guarantees uniform sampling under the Hilbert-Schmidt measure, as formally established in Ref. [59]. Let  $A \in \mathbb{R}^{N \times N}$  be a random matrix with entries independently drawn from the standard normal distribution  $\mathcal{N}(0, 1)$ . The real Ginibre ensemble

$$\rho = \frac{AA^\top}{\text{Tr}[AA^\top]} \tag{S36}$$

is a valid rebit density matrix: real, symmetric, positive semidefinite, and normalized. The following algorithm describes the practical generation of such rebit states:

---

### Algorithm 2 Sampling a Random $n$ -Rebit Density Matrix via Ginibre Ensemble

---

**Require:** Number of rebits  $n$

**Ensure:** A valid  $n$ -rebit density matrix  $\rho \in \mathbb{R}^{2^n \times 2^n}$

- 1: Let  $d \leftarrow 2^n$
  - 2: Sample  $A \in \mathbb{R}^{d \times d}$  where each  $A_{ij} \sim \mathcal{N}(0, 1)$  ▷ Real Ginibre matrix
  - 3: Compute:  $\rho \leftarrow AA^\top$  ▷ Ensure symmetry and positivity
  - 4: Normalize:  $\rho \leftarrow \rho / \text{Tr}[\rho]$  ▷ Ensure unit trace
  - 5: **return**  $\rho$
- 

The computational bottleneck in our simulations was the classification of the random samples. After obtaining a randomly sampled rebit state, we first compute the KD distribution to verify its positivity. Then, we apply the methodology described in Eqn. (S35) to determine whether the state lies within the stabilizer polytope. Sampling and state classifying 1 billion 2-qubit states took approximately 3.5 days on a x86\_64 processor with 24 physical cores and 32 logical CPUs on Intel(R) Core(TM) i9-13900K.

### VIII. PROOF OF THEOREM 2

In this Supplemental Note, we prove Theorem 2 of the main article. We need to show that KD mana is faithful, additive, and nonincreasing under free operations. We start by showing that it is faithful.

**Lemma S7.** *Let  $\rho$  be a quantum state. Then  $\mathcal{M}(\rho) = 0$  if and only if  $\rho$  is KD positive.*

*Proof.* We prove the forward direction by proving the contrapositive: if  $\rho$  is KD nonpositive, then  $\mathcal{M}(\rho) \neq 0$ . Suppose  $\rho$  is KD nonpositive. Then there must exist a  $\delta > 0$  such that there exist  $\mathbf{g}_0, \boldsymbol{\chi}_0 \in G \times \hat{G}$  such that either  $|\operatorname{Re}[Q_{\mathbf{g}_0, \boldsymbol{\chi}_0}(\rho)]| - \operatorname{Re}[Q_{\mathbf{g}_0, \boldsymbol{\chi}_0}(\rho)] \geq \delta$  or  $|\operatorname{Im}[Q_{\mathbf{g}_0, \boldsymbol{\chi}_0}(\rho)]| \geq \delta$ . This implies that there exist  $\delta, \mathbf{g}_0, \boldsymbol{\chi}_0$  such that  $|Q_{\mathbf{g}_0, \boldsymbol{\chi}_0}(\rho)| - \operatorname{Re}[Q_{\mathbf{g}_0, \boldsymbol{\chi}_0}(\rho)] \geq \delta$ .

Next, we consider minus one plus the sum of the absolute values of the entries of the KD-distribution:

$$-1 + \sum_{\mathbf{g}, \boldsymbol{\chi}} |Q_{\mathbf{g}, \boldsymbol{\chi}}(\rho)| = \sum_{\mathbf{g}, \boldsymbol{\chi}} (|Q_{\mathbf{g}, \boldsymbol{\chi}}(\rho)| - \operatorname{Re}[Q_{\mathbf{g}, \boldsymbol{\chi}}(\rho)]), \quad (\text{S37})$$

where we used that the real part of the KD distribution sums to 1. Each term in the sum on the right-hand side of Eq. (S37) is nonnegative. Since  $\rho$  is KD nonpositive, at least one of the terms in the sum must be greater than  $\delta$ . We thus find that  $-1 + \sum_{\mathbf{g}, \boldsymbol{\chi}} |Q_{\mathbf{g}, \boldsymbol{\chi}}(\rho)| \geq \delta$ . Rearranging and taking logarithms yields

$$\mathcal{M}(\rho) \geq \log(1 + \delta) \neq 0, \quad (\text{S38})$$

since  $\delta > 0$ . We have thus proven the contrapositive, establishing the result.

We now move on to the backward direction. If  $\rho$  is KD positive, then  $Q_{\mathbf{g}, \boldsymbol{\chi}}(\rho) \in [0, 1]$ . Hence  $|Q_{\mathbf{g}, \boldsymbol{\chi}}(\rho)| = Q_{\mathbf{g}, \boldsymbol{\chi}}(\rho)$ . Since the KD distribution is normalized to one, we find that  $\sum_{\mathbf{g}, \boldsymbol{\chi}} |Q_{\mathbf{g}, \boldsymbol{\chi}}(\rho)| = \sum_{\mathbf{g}, \boldsymbol{\chi}} Q_{\mathbf{g}, \boldsymbol{\chi}}(\rho) = 1$ . The result follows upon taking logarithms of both sides.  $\square$

Next, we prove that the KD mana is additive.

**Lemma S8.** *Let  $\rho, \sigma$  be quantum states. Then,  $\mathcal{M}(\rho \otimes \sigma) = \mathcal{M}(\rho) + \mathcal{M}(\sigma)$ .*

*Proof.* Let  $\mathbf{g}, \boldsymbol{\chi}$  denote the indices for the KD distribution of  $\rho$ , and let  $\mathbf{g}', \boldsymbol{\chi}'$  denote the indices for the KD distribution of  $\sigma$ . Evaluating the KD mana of  $\rho \otimes \sigma$  then yields

$$\begin{aligned} \mathcal{M}(\rho \otimes \sigma) &= \log \sum_{\mathbf{g}\mathbf{g}'\boldsymbol{\chi}\boldsymbol{\chi}'} |Q_{(\mathbf{g}, \mathbf{g}'), (\boldsymbol{\chi}, \boldsymbol{\chi}')}(\rho \otimes \sigma)| \\ &= \log \left( \sum_{\mathbf{g}\boldsymbol{\chi}} |Q_{\mathbf{g}, \boldsymbol{\chi}}(\rho)| \sum_{\mathbf{g}'\boldsymbol{\chi}'} |Q_{\mathbf{g}', \boldsymbol{\chi}'}(\sigma)| \right) \\ &= \mathcal{M}(\rho) + \mathcal{M}(\sigma), \end{aligned} \quad (\text{S39})$$

where we used Theorem 1.4 of the main paper to go from the first to the second line.  $\square$

Finally, we prove that the KD-mana is a resource monotone.

**Lemma S9.**  *$\mathcal{M}$  is nonincreasing under the free operations and is thus a monotone.*

*Proof.* We need to show that  $\mathcal{M}$  is nonincreasing under the action of the unitaries  $P_{\mathbf{g}, \boldsymbol{\chi}}, \mathbb{H}^{\otimes n}$ , and CNOT, under measurements in the computational basis, under the initialization of CSS states and under partial traces.

From Theorem 1.3, we know that the unitaries  $P_{\mathbf{g}, \boldsymbol{\chi}}, \mathbb{H}^{\otimes n}$ , CNOT permute the entries of the KD-distribution. The KD mana sums over all entries of the KD distribution, and is therefore insensitive to the ordering of the entries. Hence  $\mathcal{M}$  is invariant under the action of these unitaries.

We now show that  $\mathcal{M}$  is nonincreasing under the action of computational basis measurements. Lemma S5 shows that if the  $j$ th qubit of a state  $\rho$  is measured, then the KD distribution of the updated state  $\rho'$  is

$$Q_{\mathbf{g}, \boldsymbol{\chi}}(\rho') = \frac{1}{2} [Q_{\mathbf{g}, \boldsymbol{\chi}}(\rho) + Q_{\mathbf{g}, \boldsymbol{\chi} + \mathbf{e}_j}(\rho)], \quad (\text{S40})$$

where  $\mathbf{e}_j$  is the vector containing a 1 in the  $j$ th entry and zero everywhere else. Evaluating the sum of the absolute values of the entries of the KD distribution then yields

$$\begin{aligned}
\sum_{\mathbf{g}, \boldsymbol{\chi}} |Q_{\mathbf{g}, \boldsymbol{\chi}}(\rho')| &= \frac{1}{2} \sum_{\mathbf{g}, \boldsymbol{\chi}} |Q_{\mathbf{g}, \boldsymbol{\chi}}(\rho) + Q_{\mathbf{g}, \boldsymbol{\chi} + \mathbf{e}_j}(\rho)| \\
&\leq \frac{1}{2} \sum_{\mathbf{g}, \boldsymbol{\chi}} |Q_{\mathbf{g}, \boldsymbol{\chi}}(\rho)| + \frac{1}{2} \sum_{\mathbf{g}, \boldsymbol{\chi}} |Q_{\mathbf{g}, \boldsymbol{\chi} + \mathbf{e}_j}(\rho)| \\
&= \sum_{\mathbf{g}, \boldsymbol{\chi}} |Q_{\mathbf{g}, \boldsymbol{\chi}}(\rho)|.
\end{aligned} \tag{S41}$$

Taking logarithms of both sides then yields the desired result.

To show that  $\mathcal{M}$  is nonincreasing when CSS states are appended, note that if  $\sigma$  is a CSS state, then  $\mathcal{M}(\sigma) = 0$  by Theorem 1.2 and Theorem 2.1 of the main article. Additivity then implies that for any  $\rho$ ,  $\mathcal{M}(\rho \otimes \sigma) = \mathcal{M}(\rho)$ , showing that  $\mathcal{M}$  is constant and thus nonincreasing under the appending of CSS states.

Last, we need to show that  $\mathcal{M}$  is nonincreasing under partial traces. Without loss of generality, we will consider tracing over the first qubit of the system. We let  $g', \chi'$  denote the group element and character indexing the first qubit, and we let  $\mathbf{g}, \boldsymbol{\chi}$  denote the group element and character indexing the other qubits. We may calculate KD distribution of the partial trace of a density matrix  $\rho$  on  $n$  qubits to be

$$\begin{aligned}
Q_{\mathbf{g}, \boldsymbol{\chi}} \left( \sum_{g'} (\langle g'^{(z)} | \otimes I_{2^{n-1}}) \rho (|g'^{(z)}\rangle \otimes I_{2^{n-1}}) \right) &= \sum_{g'} \langle \mathbf{g}^{(x)} | \boldsymbol{\chi}^{(z)} \rangle (\langle g'^{(z)} | \otimes \langle \boldsymbol{\chi}^{(x)} |) \rho (|g'^{(z)}\rangle \otimes |\mathbf{g}^{(z)}\rangle) \\
&= \sum_{g' \chi'} \langle g' \mathbf{g}^{(z)} | \chi' \boldsymbol{\chi}^{(x)} \rangle \langle \chi' \boldsymbol{\chi}^{(x)} | \rho | g' \mathbf{g}^{(z)} \rangle \\
&= \sum_{g' \chi'} Q_{(g', \mathbf{g}), (\chi', \boldsymbol{\chi})}(\rho).
\end{aligned} \tag{S42}$$

Partial tracing over a qubit is therefore the same as summing over the relevant index in the KD distribution. This allows us to calculate the sum of the absolute values of the elements of a partially-traced KD distribution:

$$\begin{aligned}
\sum_{\mathbf{g}, \boldsymbol{\chi}} \left| Q_{\mathbf{g}, \boldsymbol{\chi}} \left( \sum_{g'} (\langle g'^{(z)} | \otimes I_{2^{n-1}}) \rho (|g'^{(z)}\rangle \otimes I_{2^{n-1}}) \right) \right| &= \sum_{\mathbf{g}, \boldsymbol{\chi}} \left| \sum_{g' \chi'} Q_{(g', \mathbf{g}), (\chi', \boldsymbol{\chi})}(\rho) \right| \\
&\leq \sum_{g' \mathbf{g} \chi' \boldsymbol{\chi}} |Q_{(g', \mathbf{g}), (\chi', \boldsymbol{\chi})}(\rho)|,
\end{aligned} \tag{S43}$$

where we used the triangle inequality to go from the first line to the second line. The desired result follows upon taking logarithms, completing the proof.  $\square$